Journal of Sound and Vibration (2002) **249**(2), 227–250
doi:10.1006/jsvi.2001.3804, available online at http://www.idealibrary.com on IDEAL®

FINITE ELEMENT FORMULATION AND ACTIVE VIBRATION CONTROL STUDY ON BEAMS USING SMART CONSTRAINED LAYER DAMPING (SCLD) TREATMENT

V. Balamurugan

Mechanical Systems Laboratory, Combat Vehicles Research & Development Establishment, Madras 600 054, *India. E-mail: balamuruganv_cvrde@email.com*

AND

S. Narayanan

Department of Applied Mechanics, Indian Institute of Technology, Madras 600 036, *India. E-mail: narayans@iitm.ernet.in*

(*Received* 18 *January* 2000, *and in final form* 26 *March* 2001)

This work deals with the active vibration control of beams with smart constrained layer damping (SCLD) treatment. SCLD design consists of viscoelastic shear layer sandwiched between two layers of piezoelectric sensors and actuator. This composite SCLD when bonded to a vibrating structure acts as a smart treatment. The sensor piezoelectric layer measures the vibration response of the structure and a feedback controller is provided which regulates the axial deformation of the piezoelectric actuator (constraining layer), thereby providing adjustable and significant damping in the structure. The damping offered by SCLD treatment has two components, active action and passive action. The active action is transmitted from the piezoelectric actuator to the host structure through the viscoelastic layer. The passive action is through the shear deformation in the viscoelastic layer. The active action apart from providing direct active control also adjusts the passive action by regulating the shear deformation in the structure. The passive damping component of this design eliminates spillover, reduces power consumption, improves robustness and reliability of the system, and reduces vibration response at high-frequency ranges where active damping is difficult to implement. A beam finite element model has been developed based on Timoshenko's beam theory with partially covered SCLD. The Golla–Hughes–McTavish (GHM) method has been used to model the viscoelastic layer. The dissipation co-ordinates, defined using GHM approach, describe the frequency-dependent viscoelastic material properties. Models of PCLD and purely active systems could be obtained as a special case of SCLD. Using linear quadratic regulator (LQR) optimal control, the effects of the SCLD on vibration suppression performance and control effort requirements are investigated. The effects of the viscoelastic layer thickness and material properties on the vibration control performance are investigated.

1. INTRODUCTION

Vibration and noise control of structures are essential to achieve optimal design with desirable performance. Passive damping treatments have been used extensively in many structural systems to reduce vibration response, to suppress structural instability and to eliminate vibration-induced noise. One of the methods to produce significant passive damping is constrained layer treatments. The constrained layer treatment consists of

0022-460X/02/020227 + 24 $35.00/0

a viscoelastic shear layer sandwiched between a constraining cover sheet and the structure to be damped. The vibration energy is dissipated via cyclic shearing of the viscoelastic layer. A major advantage of the constrained layer treatments is to reduce the resonance peaks without significantly altering the structural mass or stiffness. In addition, constrained layer treatments are very reliable and robust and hence are extensively used in aerospace applications. Once the damping treatments are installed, the damping cannot be adjusted.

Recently, active damping (control) has received increasing attention in the recent times especially in aerospace industries because of its ability to provide adjustable and significant damping that traditional passive damping treatments cannot. Number of researchers have studied the distributed modelling, sensing and active control using piezoelectric materials. Rao and Sunar [1] have presented an excellent review on this topic. Recently, Chen and Shen [2] have studied the optimal control of active structures with piezoelectric modal sensors and actuators. Lam and Ng [3] have studied the active control of composite plates with integrated piezoelectric sensors and actuators under various dynamic loading conditions. In spite of numerous successful research activities in this area, active damping treatments do have their limitations. For example, active damping may become unstable because of large control gains or non-collocated sensor/actuator configurations. Safety and reliability are not guaranteed for active damping systems, because malfunctions of control hardware or adverse service environments can cause the systems to lose the active damping completely or even result in instability. In addition, active damping is difficult to implement at high-frequency ranges, because the cut-off frequency of active damping is limited by control hardware capability.

From the foregoing discussions, passive and active dampings are complementary. Passive damping is reliable but not intelligent. In contrast, active damping is intelligent but not fail-safe. Naturally, a hybrid damping that is both reliable and intelligent is desirable.

Smart constrained layer damping (SCLD) treatments are hybrid designs that integrate both active and passive damping through constrained layer treatments. SCLD treatment by Shen [4, 5] consists of a viscoelastic layer sandwiched between a piezoelectric cover sheet and the host structure. Similar design suggested by Baz [6, 7] used another piezoelectric layer between the viscoelastic layer and the host structure which acts as the sensor. The vibration energy is damped due to shear deformation in the viscoelastic layer. With proper controller design, the piezoelectric cover sheet is stretched or contracted so that it always augments the passive shear deformation of the viscoelastic layer, resulting in increased damping forces acting on the structure. The strains induced in the constraining layer also develop bending moments, which further controls the vibration. Thus, two mechanisms of control operate in SCLD. Since energy is always being dissipated, it is more stable than the purely active control and also is more effective than the classical conventional passive constrained layer damping design (PCLD). In other words, it has the advantages of both the purely passive and active systems. Studies on SCLD have been carried out by a number of researchers in recent times [4–10].

In the present work, the active–passive hybrid vibration control performance due to SCLD treatment is studied on beams. A beam finite element has been formulated using Timoshenko theory, including the effect of shear deformation and rotary inertia. The viscoelastic shear layer is modelled using Golla–Hughes–McTavish (GHM) method which is a time domain approach. LQR optimal control strategy is used to obtain optimal control gains. The effect of the viscoelastic material properties (shear modulus and loss factor) on the hybrid control performance is studied and an approach to work out a viscoelastic design space for optimal performance is discussed.

2. MODELLING AND FORMULATION

A cantilever beam with partially treated enhanced smart constrained layer (Figure 1(a)) is considered similar to the one in reference [10]. A beam finite element has been formulated with Timoshenko's beam theory with the following assumptions: (1) the transverse displacement w is assumed to be the same in all the layers, (2) the Young's modulus of the viscoelastic material is negligible when compared with that of the beam and piezoelectric layer, (3) linear theories are used, (4) perfect continuity without any slip is assumed at the interfaces, (5) the applied voltage is assumed to be uniform along the beam.

The beam model with the partially covered SCLD treatment (Figure 1(c)) is divided into two types of elements (1) beam elements with SCLD treatment and (2) plain beam elements.

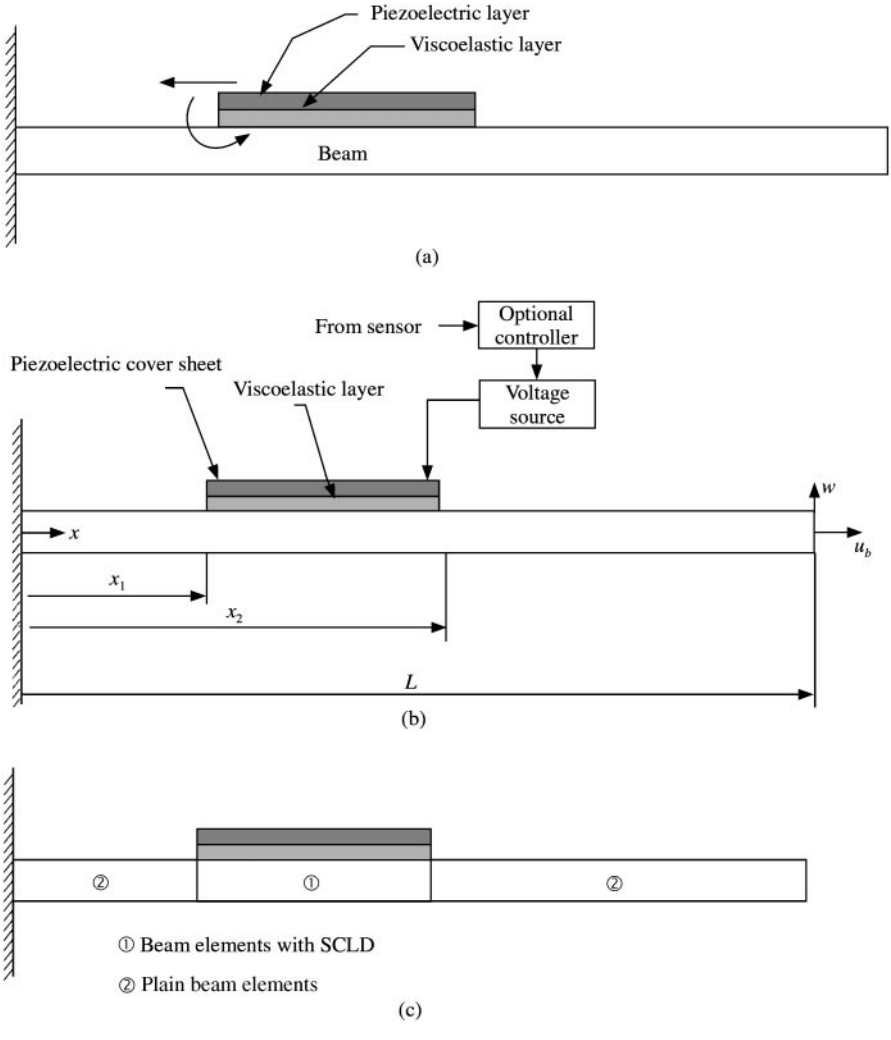

Figure 1. (a,b) Cantilever beam with partially covered SCLD treatment; (c) Finite element idealization of a cantilever beam with partially covered SCLD treatment.

2.1. BEAM ELEMENTS WITH SCLD TREATMENT

2.1.1. *Kinematic relationships*

The geometry and deformation of the beam with SCLD treatment is as shown in Figure 2. The axial displacement of the neutral axis of the piezoelectric layer, the viscoelastic shear layer and the beam are u_c, u_s and u_b respectively. w and θ denote the transverse displacement and rotation respectively. From Figure 2, the shear strain γ of the viscoelastic shear layer is given by

$$\gamma = \theta - \psi, \tag{1}$$

where ψ is the rotational angle of the viscoelastic layer. Assuming perfect bonding conditions the following kinematics relations could be derived:

$$u_s = u_b - \frac{t_b}{2}\theta - \frac{t_s}{2}\psi, \qquad u_c = u_b - \frac{t_b + t_c}{2}\theta - t_s\psi, \tag{2, 3}$$

where t_b, t_c and t_s are the thickness of beam, the piezoelectric layer, and the viscoelastic layer respectively.

2.1.2. *Shape functions*

The transverse displacement w, the rotation θ, the axial displacement u_b and the shear angle γ are interpolated by using linear polynomial in x defined over the element length L_e. The local nodal displacements for the SCLD elements (Figure 3) are given by

$$\{q\}_e = [u_1 \;\; w_1 \;\; \theta_1 \;\; \gamma_1 \;\; u_2 \;\; w_2 \;\; \theta_2 \;\; \gamma_2]^{\mathrm{T}}. \tag{4}$$

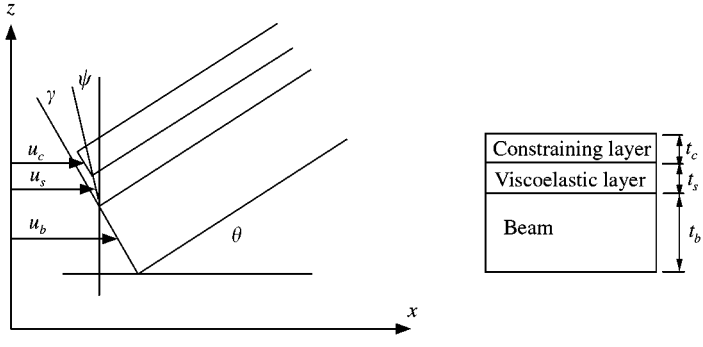

Figure 2. The geometry and deformation of a SCLD-treated beam.

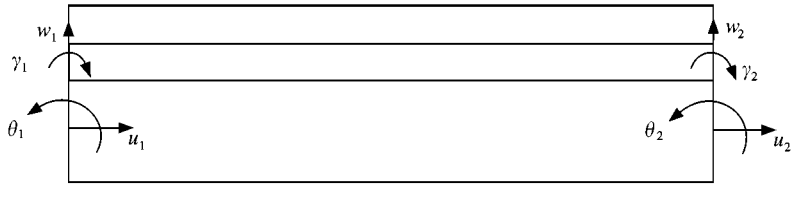

Figure 3. Nodal displacements of SCLD-treated beam.

The axial displacement, transverse displacement and shear angle are expressed in terms of the nodal displacements by finite element shape functions as

$$u_b = [N_u(x)]\{q\}_e, \quad w = [N_w(x)]\{q\}_e, \quad \theta = [N_\theta(x)]\{q\}_e, \quad \gamma = [N_\gamma(x)]\{q\}_e, \tag{5}$$

where the shape functions are given by

$$[N_u(x)]^{\mathrm{T}} = \begin{bmatrix} 1-\frac{x}{L_e} \\ 0 \\ 0 \\ 0 \\ \frac{x}{L_e} \\ 0 \\ 0 \\ 0 \end{bmatrix}, \quad [N_w(x)]^{\mathrm{T}} = \begin{bmatrix} 0 \\ 1-\frac{x}{L_e} \\ 0 \\ 0 \\ 0 \\ \frac{x}{L_e} \\ 0 \\ 0 \end{bmatrix}, \quad [N_\theta(x)]^{\mathrm{T}} = \begin{bmatrix} 0 \\ 0 \\ 1-\frac{x}{L_e} \\ 0 \\ 0 \\ 0 \\ \frac{x}{L_e} \\ 0 \end{bmatrix}, \quad [N_\gamma(x)]^{\mathrm{T}} = \begin{bmatrix} 0 \\ 0 \\ 0 \\ 1-\frac{x}{L_e} \\ 0 \\ 0 \\ 0 \\ \frac{x}{L_e} \end{bmatrix}. \tag{6}$$

From equations (1)–(3), we have

$$u_c = u_b - h\theta + t_s\gamma = \{1 \quad -h \quad t_s\} \begin{bmatrix} [N_u] \\ [N_\theta] \\ [N_\gamma] \end{bmatrix} \{q\}_e, \tag{7}$$

$$u_c = u_b - \frac{t_b + t_s}{2}\theta + \frac{t_s}{2}\gamma = \left\{1 \quad -\frac{t_b + t_s}{2} \quad \frac{t_s}{2}\right\} \begin{bmatrix} [N_u] \\ [N_\theta] \\ [N_\gamma] \end{bmatrix} \{q\}_e, \tag{8}$$

where

$$h \equiv t_s + \frac{t_b + t_c}{2}. \tag{9}$$

2.1.3. *Beam layer*

The potential energy of the beam due to bending is

$$\frac{1}{2} E_b I_b \int_0^{L_e} \left(\frac{\partial\theta}{\partial x}\right)^2 \mathrm{d}x = \frac{1}{2} E_b I_b \{q\}_e^{\mathrm{T}} \int_0^{L_e} [N'_\theta]^{\mathrm{T}} [N'_\theta] \,\mathrm{d}x \,\{q\}_e$$

$$= \frac{1}{2} \{q\}_e^{\mathrm{T}} [K_{wbb}] \{q\}_e. \tag{10}$$

The potential energy of the beam due to transverse shear is

$$\frac{1}{2} G_b A_b k_\alpha \int_0^{L_e} \left(\theta - \frac{\partial w}{\partial x}\right)^2 \mathrm{d}x = \frac{1}{2} G_b A_b k_\alpha \{q\}_e^{\mathrm{T}} \int_0^{L_e} \begin{bmatrix} [N_\theta] \\ [N'_w] \end{bmatrix}^{\mathrm{T}} \begin{Bmatrix} 1 \\ -1 \end{Bmatrix} \{1 \quad -1\} \begin{bmatrix} [N_\theta] \\ [N'_w] \end{bmatrix} \mathrm{d}x \,\{q\}_e$$

$$= \frac{1}{2} \{q\}_e^{\mathrm{T}} [K_{wbs}] \{q\}_e, \tag{11}$$

where E_b, G_b, I_b and A_b are Young's modulus of the beam material, shear modulus of the beam material, moment of inertia and are a of the beam cross-section respectively. k_α is the shear correction factor (usually equal to 5/6). In the evaluation of transverse shear energy,

reduced integration is used to eliminate shear locking [15]. The potential energy of the beam due to extension is

$$\frac{1}{2}E_b A_b \int_0^{L_e}\left(\frac{\partial u_b}{\partial x}\right)^2 \mathrm{d}x = \frac{1}{2}E_b A_b \{q\}_e^{\mathrm{T}} \int_0^{L_e} [N_u']^{\mathrm{T}} [N_u'] \,\mathrm{d}x \,\{q\}_e$$

$$= \frac{1}{2}\{q\}_e^{\mathrm{T}} [K_{ub}] \{q\}_e. \tag{12}$$

The kinetic energy of the beam associated with the transverse motion including rotary inertia is

$$\int_0^{L_e}\left[\frac{1}{2}\rho_b A_b\left(\frac{\partial w}{\partial t}\right)^2 + \frac{1}{2}\rho_b I_b\left(\frac{\partial \theta}{\partial t}\right)^2\right]\mathrm{d}x = \frac{1}{2}\rho_b \{\dot{q}\}_e^{\mathrm{T}} \int_0^{L_e} (A_b [N_w]^{\mathrm{T}} [N_w] + I_b [N_\theta]^{\mathrm{T}} [N_\theta])\,\mathrm{d}x \,\{\dot{q}\}_e^{\mathrm{T}}$$

$$= \frac{1}{2}\{\dot{q}\}_e^{\mathrm{T}} [M_{wb}] \{\dot{q}\}_e. \tag{13}$$

The kinetic energy of the beam associated with axial motion is

$$\frac{1}{2}\rho_b A_b \int_0^{L_e}\left(\frac{\partial u_b}{\partial t}\right)^2 \mathrm{d}x = \frac{1}{2}\rho_b A_b \{\dot{q}\}_e^{\mathrm{T}} \int_0^{L_e} [N_u]^{\mathrm{T}} [N_u] \,\mathrm{d}x \,\{\dot{q}\}_e$$

$$= \frac{1}{2}\{\dot{q}\}_e^{\mathrm{T}} [M_{ub}] \{\dot{q}\}_e. \tag{14}$$

2.1.4. *Piezoelectric layer*

For one-dimensional structures with uni-axial loading, the constitutive equation of the piezoelectric materials [11] can be written as

$$\begin{bmatrix} E \\ D \end{bmatrix} = \begin{bmatrix} S_{11}^E & d_{31} \\ d_{31} & \varepsilon_{33}^{\mathrm{T}} \end{bmatrix} \begin{bmatrix} \sigma \\ E \end{bmatrix}, \tag{15}$$

where D is the electrical displacement (charge/area in the beam vertical direction), E is the electric field (voltage/length along vertical direction), E is the mechanical strain in the x direction, and σ is the mechanical stress in the x direction. S_{11}^E is the elastic compliance constant, $\varepsilon_{33}^{\mathrm{T}}$ is the dielectric constant, and d_{31} is the piezoelectric strain constant. Based on the above constitutive equation, the stress–strain relation is given by

$$\sigma = E_c(E - d_{31}\,E), \tag{16}$$

where

$$E_c = C_{11}^E = \frac{1}{S_{11}^E}, \quad E = \frac{V(t)}{t_c}. \tag{17}$$

The virtual work done by the induced strain (force) in the actuator is

$$\delta W_c = \int_0^{L_e} E_c d_{31} b V(t) \delta\left(\frac{\partial u_c}{\partial x}\right)\mathrm{d}x = E_c d_{31} b V(t)(\delta u_c|_{x=L_c} - \delta u_c|_{x=0})$$

$$= E_c d_{31} b V(t) \{\delta q\}_e^{\mathrm{T}} \left(\begin{bmatrix} [N_u(L_e)] \\ [N_\theta(L_e)] \\ [N_\gamma(L_e)] \end{bmatrix}^{\mathrm{T}} \begin{Bmatrix} 1 \\ -h \\ t_s \end{Bmatrix} - \begin{bmatrix} [N_u(0)] \\ [N_\theta(0)] \\ [N_\gamma(0)] \end{bmatrix}^{\mathrm{T}} \begin{Bmatrix} 1 \\ -h \\ t_s \end{Bmatrix} \right)$$

$$= \{\delta q\}_e^{\mathrm{T}} E_c d_{31} b V(t) \times \{-1 \;\; 0 \;\; h \;\; -t_s \;\; 1 \;\; 0 \;\; -h \;\; t_s\}^{\mathrm{T}} = \{\delta q\}_e^{\mathrm{T}} \{P_c\}_e V(t), \tag{18}$$

where $[P_c\}_e$ is the elemental piezoelectric force vector which maps the applied actuator voltage to induced displacements. $V(t)$ is the voltage applied to the constraining piezoelectric layer. The potential energy of the piezoelectric layer due to bending is

$$\frac{1}{2}E_c I_c \int_0^{L_e}\left(\frac{\partial\theta}{\partial x}\right)^2 \mathrm{d}x = \frac{1}{2}E_c I_c \{q\}_e^{\mathrm{T}} \int_0^{L_e} [N'_\theta]^{\mathrm{T}}[N'_\theta]\,\mathrm{d}x\,\{q\}_e$$

$$= \frac{1}{2}\{q\}_e^{\mathrm{T}}[K_{wcb}]\{q\}_e. \tag{19}$$

The potential energy of the piezoelectric layer due to transverse shear is

$$\frac{1}{2}G_c A_c k_\alpha \int_0^{L_e}\left(\theta - \frac{\partial w}{\partial x}\right)^2 \mathrm{d}x = \frac{1}{2}G_c A_c k_\alpha \{q\}_e^{\mathrm{T}} \int_0^{L_e}\begin{bmatrix}[N_\theta]\\ [N'_w]\end{bmatrix}^{\mathrm{T}}\begin{Bmatrix}1\\ -1\end{Bmatrix}\{1 \quad -1\}\begin{bmatrix}[N_\theta]\\ [N'_w]\end{bmatrix}\mathrm{d}x\,\{q\}_e$$

$$= \frac{1}{2}\{q\}_e^{\mathrm{T}}[K_{wcs}]\{q\}_e, \tag{20}$$

where E_c, G_c, I_c and A_c are Young's modulus of the piezoelectric material, shear modulus of the piezoelectric material, moment of inertia and area of the piezoelectric layer cross-section respectively. As mentioned earlier, the shear energy terms are obtained by reduced integration. The potential energy of the piezoelectric layer due to extension is

$$\frac{1}{2}E_c A_c \int_0^{L_e}\left(\frac{\partial u_c}{\partial x}\right)^2 \mathrm{d}x = \frac{1}{2}E_c A_c \{q\}_e^{\mathrm{T}} \int_0^{L_e}\begin{bmatrix}[N'_u]\\ [N'_\theta]\\ [N'_\gamma]\end{bmatrix}^{\mathrm{T}}\begin{Bmatrix}1\\ -h\\ t_s\end{Bmatrix}\{1 \quad -h \quad t_s\}\begin{bmatrix}[N'_u]\\ [N'_\theta]\\ [N'_\gamma]\end{bmatrix}^{\mathrm{T}}\mathrm{d}x\,\{q\}_e$$

$$= \frac{1}{2}\{q\}_e^{\mathrm{T}}[K_{uc}]\{q\}_e, \tag{21}$$

where A_c is the area of cross-section of the piezoelectric layer. The kinetic energy of the piezoelectric layer associated with transverse motion is

$$\int_0^{L_e}\left[\frac{1}{2}\rho_c A_c\left(\frac{\partial w}{\partial t}\right)^2 + \frac{1}{2}\rho_c I_c\left(\frac{\partial\theta}{\partial t}\right)^2\right]\mathrm{d}x = \frac{1}{2}\rho_c\{\dot{q}\}_e^{\mathrm{T}}\int_0^{L_e}(A_c[N_w]^{\mathrm{T}}[N_w] + I_c[N_\theta]^{\mathrm{T}}[\mathrm{N}_\theta])\,\mathrm{d}x(\dot{q})_e$$

$$= \frac{1}{2}\{\dot{q}\}_e^{\mathrm{T}}[M_{wc}]\{\dot{q}\}_e, \tag{22}$$

where ρ_c is the density of the piezoelectric material. The kinetic energy of the piezoelectric layer associated with axial motion is

$$\frac{1}{2}\rho_c A_c \int_0^{L_e}\left(\frac{\partial u_c}{\partial t}\right)^2 \mathrm{d}x = \frac{1}{2}\rho_c A_c \{\dot{q}\}_e^{\mathrm{T}} \int_0^{L_e}\begin{bmatrix}[N_u]\\ [N_\theta]\\ [N_\gamma]\end{bmatrix}^{\mathrm{T}}\begin{Bmatrix}1\\ -h\\ t_s\end{Bmatrix}\{1 \quad -h \quad t_s\}\begin{bmatrix}[N_u]\\ [N_\theta]\\ [N_\gamma]\end{bmatrix}\mathrm{d}x\,\{\dot{q}\}_e$$

$$= \frac{1}{2}\{\dot{q}\}_e^{\mathrm{T}}[M_{uc}]\{\dot{q}\}_e. \tag{23}$$

2.1.5. *Viscoelastic layer*

The kinetic energy of the viscoelastic layer associated with transverse motion is

$$\int_0^{L_e}\left[\frac{1}{2}\rho_s A_s\left(\frac{\partial w}{\partial t}\right)^2 + \frac{1}{2}\rho_s I_s\left(\frac{\partial\theta}{\partial t}\right)^2\right]\mathrm{d}x = \frac{1}{2}\rho_s\{\dot{q}\}_s^{\mathrm{T}}\int_0^{L_e}(A_s[N_w]^{\mathrm{T}}[N_w] + I_s[N_\theta]^{\mathrm{T}}[\mathrm{N}_\theta])\,\mathrm{d}x\{\dot{q}\}_e$$

$$= \frac{1}{2}\{\dot{q}\}_e^{\mathrm{T}}[M_{ws}]\{\dot{q}\}_e, \tag{24}$$

where ρ_s, I_s and A_s are the density, moment of inertia and area of cross-section of the viscoelastic layer. The kinetic energy of the viscoelastic layer associated with axial motion is

$$\frac{1}{2}\rho_s A_s \int_0^{L_e} \left(\frac{\partial u_s}{\partial t}\right)^2 \mathrm{d}x = \frac{1}{2}\rho_s A_s \{\dot{q}\}_e^{\mathrm{T}} \int_0^{L_e} \begin{bmatrix} [N_u] \\ [N_\theta] \\ [N_\gamma] \end{bmatrix}^{\mathrm{T}} \begin{Bmatrix} 1 \\ -\frac{t_b + t_s}{2} \\ \frac{t_s}{2} \end{Bmatrix} \begin{Bmatrix} 1 & -\frac{t_b + t_s}{2} & \frac{t_s}{2} \end{Bmatrix} \begin{bmatrix} [N_u] \\ [N_\theta] \\ [N_\gamma] \end{bmatrix} \mathrm{d}x \{\dot{q}\}_e$$

$$= \frac{1}{2}\{\dot{q}\}_e^{\mathrm{T}} [M_{us}] \{\dot{q}\}_e. \tag{25}$$

For one-dimensional structures, the constitutive equation for viscoelastic materials could be represented in the following Stieltjes integral form [10]

$$\tau(x, t) = G \circ \gamma \equiv \int_{-\infty}^{t} G(t - \tau) \frac{\partial \gamma}{\partial \tau}(x, \tau)\, \mathrm{d}\tau, \tag{26}$$

where $G(t)$ is the relaxation function of viscoelastic material (the stress response to a unit-step strain input). This stress relaxation represents energy loss from the material and hence damping.

The Golla–Hughes–Mctavish (GHM) method [13, 14] is employed to analyze equation (26) in the time domain [10]. The GHM method represents the material modulus function as a series of mini-oscillator terms in the Laplace domain [12]

$$s\tilde{G}(\mathrm{s}) = \kappa \left[1 + \sum_{r=1}^{n} \alpha_r \frac{s^2 + 2\hat{\zeta}_r \hat{\omega}_r s}{s^2 + 2\hat{\zeta}_r \hat{\omega}_r s + \hat{\omega}_r^2}\right]. \tag{27}$$

The factor κ corresponds to the equilibrium value of the modulus—the final value of the relaxation function $G(t)$. Each mini-oscillator term is a second order rational function involving three positive constants $\{\alpha_r, \hat{\omega}_r, \hat{\zeta}_r\}$ which are weighting on the GHM dissipation co-ordinate, the natural frequency in GHM dissipation co-ordinate and the damping factor in GHM dissipation co-ordinate respectively. These constants govern the shape of the modulus function over the complex s-domain. the GHM parameters κ and α can be related to the shear modulus and the loss factor of viscoelastic materials. From a single-term GHM expression, we can obtain the following time-domain pair:

$$G \circ \gamma = (\kappa + \alpha\kappa)\gamma - \alpha\kappa z, \tag{28}$$

$$\left(\alpha\kappa \frac{1}{\hat{\omega}^2}\right)\ddot{z} + \left(\alpha\kappa \frac{2\hat{\zeta}}{\hat{\omega}}\right)\dot{z} - \alpha\kappa\gamma + \alpha\kappa z = 0, \tag{29}$$

where z is the dissipation co-ordinate which may be expressed as follows:

$$z = N_z(x)\{z\} = \begin{bmatrix} 1 - \frac{x}{L_e} & \frac{x}{L_e} \end{bmatrix} \begin{Bmatrix} z_1 \\ z_2 \end{Bmatrix}. \tag{30}$$

The virtual work done by the viscoelastic layer is therefore,

$$\delta W_s = -A_s \int_0^{L_e} (G \circ \gamma)\delta\gamma\, \mathrm{d}x = -A_s \{\delta q\}_e^{\mathrm{T}} \int_0^{L_e} [N_\gamma]^{\mathrm{T}} (G \circ \gamma)\, \mathrm{d}x \tag{31}$$

$$= -A_s \{\delta q^e\}^{\mathrm{T}} \left((\kappa + \alpha\kappa) \int_0^{L_e} [N_\gamma]^{\mathrm{T}} [N_\gamma]\, \mathrm{d}x \{q\}_e - \alpha\kappa \int_0^{L_e} [N_\gamma]^{\mathrm{T}} [N_z]\, \mathrm{d}x \{z\}\right)$$

$$\delta W_s = -\{\delta q\}_e^{\mathrm{T}} [K_s] \{q\}_e + \{\delta q^e\}^{\mathrm{T}} [K_{qz}] \{z\} \tag{32}$$

and

$$[M_z]\{\ddot{z}\} + [C_z]\{\dot{z}\} - [K_{zq}]\{q\}_e + [k_z]\{z\} = 0, \tag{33}$$

where

$$[K_s] = A_s(\kappa + \alpha\kappa)\int_0^{L_e} [N_\gamma]^{\mathrm{T}}[N_\gamma]\,\mathrm{d}x, \qquad [K_{qz}] = A_s\alpha\kappa\int_0^{L_e} [N_\gamma]^{\mathrm{T}}[N_z]\,\mathrm{d}x, \tag{34, 35}$$

$$[K_{zq}] = A_s\,\alpha\kappa\int_0^{L_e} [N_z]^{\mathrm{T}}[N_\gamma]\,\mathrm{d}x = [K_{qz}]^{\mathrm{T}}, \tag{36}$$

$$[K_z] = A_s\,\alpha\kappa\int_0^{L_e} [N_z]^{\mathrm{T}}[N_z]\,\mathrm{d}x, \qquad [M_z] = A_s\alpha\kappa\,\frac{1}{\hat{\omega}^2}\int_0^{L_e} [N_z]^{\mathrm{T}}[N_z]\,\mathrm{d}x, \tag{37, 38}$$

$$[C_z] = A_s\,\alpha\kappa\,\frac{2\hat{\zeta}}{\hat{\omega}}\int_0^{L_e} [N_z]^{\mathrm{T}}[N_z]\,\mathrm{d}x. \tag{39}$$

The above formulation will ensure the system stiffness matrix to be symmetric.

2.1.6. *Mass, damping and stiffness matrices of SCLD-treated elements*

The final mass, damping, and stiffness matrices for a single SCLD element corresponding to $\{q\}_e$, can be expressed as follows:

$$[M]_e = [M_{wb}] + [M_{wc}] + [M_{ws}] + [M_{ub}] + [M_{uc}] + [M_{us}], \tag{40}$$

$$[K]_e = [K_{wbb}] + [K_{wbs}] + [K_{wcb}] + [K_{wcs}] + [K_{ub}] + [K_{uc}] + [K_{us}] + [K_s]. \tag{41}$$

The matices corresponding to both $\{q\}_e$ and $\{z\}$ are $[K_{qz}]$ and $[K_{zq}]$. The matrices corresponding to $\{z\}$ are $[M_z]$, $[C_z]$ and $[K_z]$.

The mass and stiffness matrices have a dimension 6×6 for the elements in the plain beam regions, without piezoelectric, viscoelastic layers and edge elements. The virtual work done by the distributed external disturbance force is given by

$$\delta W_d = \int_0^{L_e} f(x, t)\,\delta w(x, t)\,\mathrm{d}x = \{\delta q^e\}^{\mathrm{T}}\{f_d\}. \tag{42}$$

It is usually more convenient to define nodes at the point of application of any discrete forces, and to consider the effects of such forces at the global level.

3. EQUATIONS OF MOTION OF BEAM WITH PARTIALLY COVERED SCLD TREATMENT

Using Hamilton's principle one can write

$$\int_{t_1}^{t_2} [\delta T_e - \delta U_e + \delta W_e]\,\mathrm{d}t = 0, \tag{43}$$

where T_e, U_e and W_e are the elemental kinetic energy, potential energy and virtual work respectively. From equation (43), we can write the equations of motion for an element as

$$\begin{bmatrix} [M]_e & [0] \\ [0] & [M_z] \end{bmatrix}\begin{Bmatrix} \{\ddot{q}\}_e \\ \{\ddot{z}\}_e \end{Bmatrix} + \begin{bmatrix} [0] & [0] \\ [0] & [C_z] \end{bmatrix}\begin{Bmatrix} \{\dot{q}\}_e \\ \{\dot{z}\}_e \end{Bmatrix} + \begin{bmatrix} [K]_e & -[K_{qz}] \\ -[K_{zq}] & [K_z] \end{bmatrix}\begin{Bmatrix} \{q\}_e \\ \{z\}_e \end{Bmatrix} = \begin{Bmatrix} \{P_c\}_e\{V(t)\}_e + \{f_d\}_e \\ \{0\} \end{Bmatrix}. \tag{44}$$

The elemental dissipation co-ordinates $\{z\}_e$ are considered as additional degrees of freedom per node. The global equations of motion can be obtained by assembling the elemental equations and are given by

$$[M]\{\ddot{q}\} + [C]\{\dot{q}\} + [K]\{q\} = \{P_c\}\{V(t)\} + \{f_d\}, \tag{45}$$

where $\{q\}$, $\{\dot{q}\}$ and $\{\ddot{q}\}$ are the global displacement, the velocity and the acceleration vectors respectively (including GHM dissipation co-ordinates). $[M]$, $[C]$ and $[K]$ are the mass, damping and stiffness matrices. $\{P_c\}$ is the piezoelectric force vector which maps the applied actuator voltage to the induced displacements and $\{f_d\}$ is the vector representing disturbance forces. Note that the piezoelectric-induced force results in boundary actions at the ends of the piezoelectric layer due to the force cancellation at common nodes, when continuity between elements is enforced.

In the present study, in addition to the viscoelastic damping as in the above formulation, internal structural damping is also included via Rayleigh damping as

$$[C_b] = \hat{a}[M_b] + \hat{b}[K_b], \tag{46}$$

where $[M_b]$ and $[K_b]$ are submatrices of $[M]$ and $[K]$, respectively, from which the parts corresponding to the GHM dissipation co-ordinates are removed. Constants $\hat{a}$ and $\hat{b}$ can be usually obtained from experimental results [15].

4. MODAL ANALYSIS AND STATE-SPACE FORMULATION

For most structural systems under practical loading conditions, the vibration response is governed by only the first few modes. Hence, mode superposition method is used to obtain an approximate reduced order dynamic model of the system with uncoupled equations of motion in modal co-ordinates. Assuming that the system response is governed by the first r modes of the system, the displacement $\{q(t)\}$ could be approximated by

$$\{q\} \approx \sum_{j=1}^{r} \phi_j \eta_j = [\hat{\Phi}]\{\eta\}, \tag{47}$$

where $[\hat{\Phi}]$ is the truncated modal matrix (of the associated undamped free-vibration problem), given by

$$[\hat{\Phi}] = [\phi_1, \ldots, \phi_r] \quad (r < n) \tag{48}$$

and $[\eta(t)\}$ are the modal co-ordinates, and r is the number of retained modes.

Using the approximation for $\{q\}$ given in equation (48), the equation of motion (45) could be transformed to the reduced modal space from as below.

$$[\bar{M}]\{\ddot{\eta}\} + [\bar{C}]\{\dot{\eta}\} + [\bar{K}]\{\eta\} = \{\bar{P}_c\}\{V(t)\} + \{\bar{f}_d\}, \tag{49}$$

where

$$[\bar{M}] = [\hat{\Phi}]^{\mathrm{T}}[M][\hat{\Phi}], \quad [\bar{C}] = [\hat{\Phi}]^{\mathrm{T}}[C][\hat{\Phi}], \quad [\bar{K}] = [\hat{\Phi}]^{\mathrm{T}}[K][\hat{\Phi}]$$

are $(r \times r)$ diagonal matrices because of the orthogonality of the mode shapes (eigenvectors) with respect to the mass and stiffness matrices, and

$$\{\bar{P}_c\} = [\hat{\Phi}]^{\mathrm{T}}[P_c\}, \quad \{\bar{f}_d\} = [\hat{\Phi}]^{\mathrm{T}}\{f_d\}.$$

Equation (49) can be written as

$$[\ddot{\eta}] = -[\bar{M}]^{-1}[\bar{K}]\{\eta\} - [\bar{M}]^{-1}[\bar{C}]\{\dot{\eta}\} + [\bar{M}]^{-1}\{\bar{P}_c\}\{V(t)\} + [\bar{M}]^{-1}\{\bar{f}_d\}. \tag{50}$$

Introducing the state-space variable $[\xi]$ as

$$[\xi] = \begin{Bmatrix} \dot{\eta} \\ \eta \end{Bmatrix}. \tag{51}$$

The system dynamics given by equation (50) can be written in a state-space from as

$$[\dot{\xi}] = [A]\{\xi\} + [B]\{u\} + [\hat{B}]\{u_d\}, \tag{52}$$

where $[A]$ is the system matrix, $[B]$ is the control matrix and $[\hat{B}]$ is the disturbance matrix, which are given by

$$[A] = \begin{bmatrix} -[\bar{M}]^{-1}[\bar{C}] & -[\bar{M}]^{-1}[\bar{K}] \\ [I] & [0] \end{bmatrix}, \quad [B] = \begin{bmatrix} [\bar{M}]^{-1}\{\bar{P}_c\} \\ [0] \end{bmatrix}, \quad [\hat{B}] = \begin{bmatrix} [\bar{M}]^{-1}\{\bar{f}_d\} \\ [0] \end{bmatrix},$$

where $\{u_d\}$ is the disturbance input vector and $\{u\} = V(t)$ is the control input. The output equation could be written in physical co-ordinates as

$$\{y\} = [C_o]\{q\}, \tag{53}$$

where $[C_o]$ is the output matrix. On transforming to modal co-ordinates and then to state-space co-ordinates, equation (53) becomes

$$\{\bar{y}\} = [[0], \quad [C_o][\hat{\Phi}]]\{\xi\} = [\bar{C}_o]\{\xi\}. \tag{54}$$

The state-space model of the system dynamics represented by equations (53) and (54) is used for vibration control study. It could be noted that the models of PCLD and purely active systems could be obtained as a special case of SCLD model by imposing appropriate assumptions.

5. OPTIMAL CONTROL LAW

Linear quadratic regulator theory (LQR) optimal control theory [16, 17] is used to determine the active control gains. The cost function is given by

$$J = \int_0^\infty (\{\bar{y}\}^{\mathrm{T}}[Q]\{\bar{y}\} + \{u\}^{\mathrm{T}}[R]\{u\})\,\mathrm{d}t, \tag{55}$$

where $[Q]$ and $[R]$ are the semi-positive-definite and positive-definite weighting matrices on the outputs and control inputs respectively. In our case, larger (relatively) elements in $[Q]$ mean that we demand more vibration suppression ability from the controller, while larger R elements mean one's interest is in limiting the control effort (voltage). Assuming full state feedback, the control law is given by

$$\{u\} = -[K_c]\{\xi\}, \tag{56}$$

where $[K_c]$ is the control gain given by

$$[K_c] = [R]^{-1}[B]^{\mathrm{T}}[P]. \tag{57}$$

$[P]$ satisfies the Riccati equation

$$[A]^{\mathrm{T}}[P] + [P][A] - [P][B][R]^{-1}[B]^{\mathrm{T}}[P] + [C_0]^{\mathrm{T}}[Q]\{C_0] = 0. \tag{58}$$

The closed-loop system dynamics is given by

$$\{\dot{\xi}\} = ([A] - [B][K_c])\{\xi\} + [\hat{B}]\{u_d\} = [A_{cl}]\{\xi\} + [\hat{B}]\{u_d\}. \tag{59}$$

TABLE 1

Material properties and other system parameters

$\hat{a}$	0·64	d_{31}	-175×10^{-12} m/V
$\hat{b}$	$1{\cdot}2\times10^{-6}$	k_{eq}	10^8 N/m^2
E_b	$7{\cdot}1\times10^{10}$ N/m^2	L	300 mm
E_c	$6{\cdot}49\times10^{10}$ N/m^2	x_1	30 min
κ	5×10^5 N/m^2	x_2	130 mm
ρ_b	2700 kg/m^3	t_b	3 mm
ρ_c	7600 kg/m^3	t_c	1 mm
ρ_s	1250 kg/m^3	t_s	0·25 mm
α	1·0	b	15 mm
$\hat{\omega}$	1000 rad/s	Q	10^{11}
$\hat{\varsigma}$	4·0	R	1·0

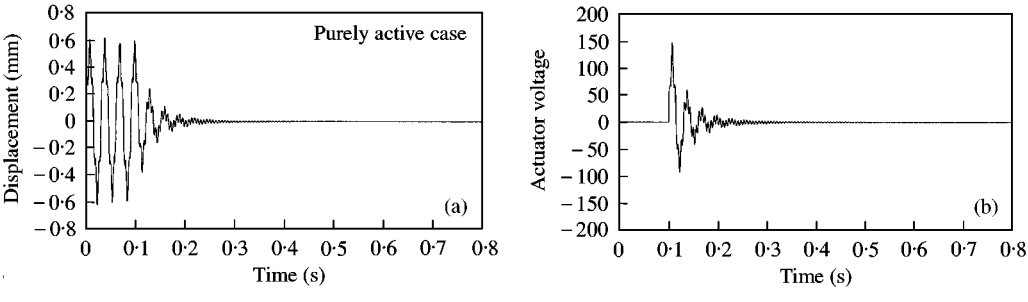

Figure 4. Tip displacement and actuator voltage of the beam with purely active control.

6. RESULTS AND DISCUSSION

For vibration control studies, a SCLD-treated cantilever beam of dimensions 300 mm × 15 mm × 3 mm is considered with the viscoelastic layer and piezoelectric cover sheet of 100 mm × 15 mm at 30 mm from the fixed end. Table 1 indicates the system parameters of the case studies considered for the different cases unless otherwise specifically stated. An impact load of 1·0 N is applied at the free end of the cantilever beam for 1 ms duration. Controller is assumed to be switched on after 0·1 s. Figures 4–7 show the vibration control performance and control effort for purely active case and PCLD and SCLD for different values of κ (final value of the relaxation function of viscoelastic material which is also related to shear modulus). It could be observed from the figures that with higher κ we could achieve better vibration control performance. In the present case with $\kappa = 10^8$, we could achieve vibration control performance matching the purely active case. It can be noted that the actuator voltages shown in Figures 4–7 are of the order of 100–150 V and the thickness of the PZT actuator is 1 mm. Hence, the field applied to the actuator is 100–150 V/mm which is less compared to the breakdown voltages for such PZT materials. Figure 8 indicates the vibration control performance of the SCLD-treated beam subjected to a sinusoidal load of 0·1 sin(250t) at the tip, the control parameters Q and R being 10^{12} and 1 respectively. In this case it can also be noted that with $\kappa = 10^8$, we could achieve vibration control performance matching the purely active case. In this case, the controller is switched on after 2 s. It can be noted that, the beat-like phenomenon which is observed in the uncontrolled case is due to the superposition of the transient response which is at the natural frequency (in this case 206 rad/s) and the steady state response which is 250 rad/s.

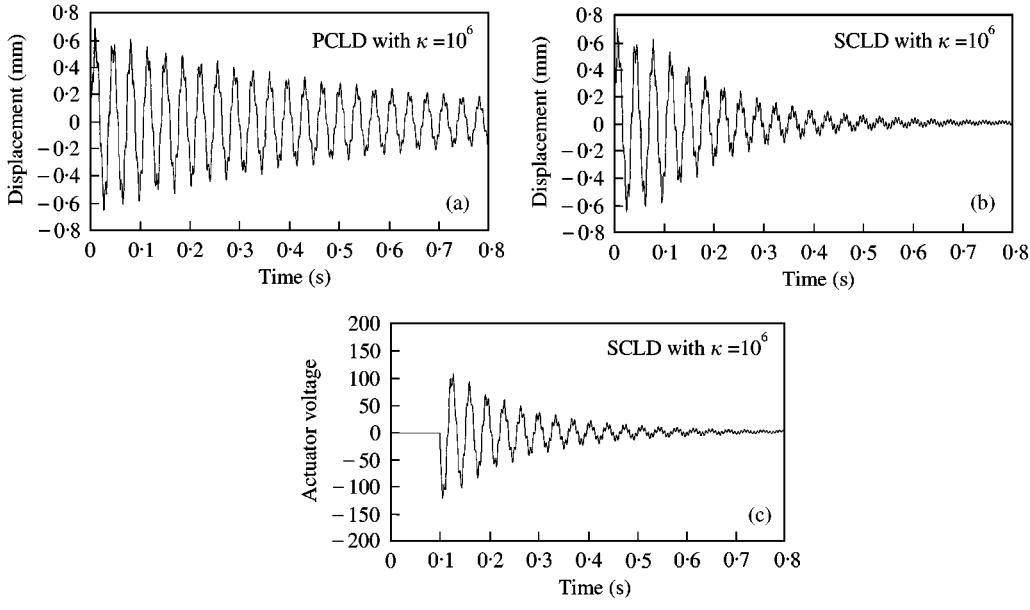

Figure 5. Tip displacement and actuator voltage of the beam with PCLD and SCLD (with $\kappa = 10^6$ N/m^2), when subjected to an impact load of 1·0 N at the tip.

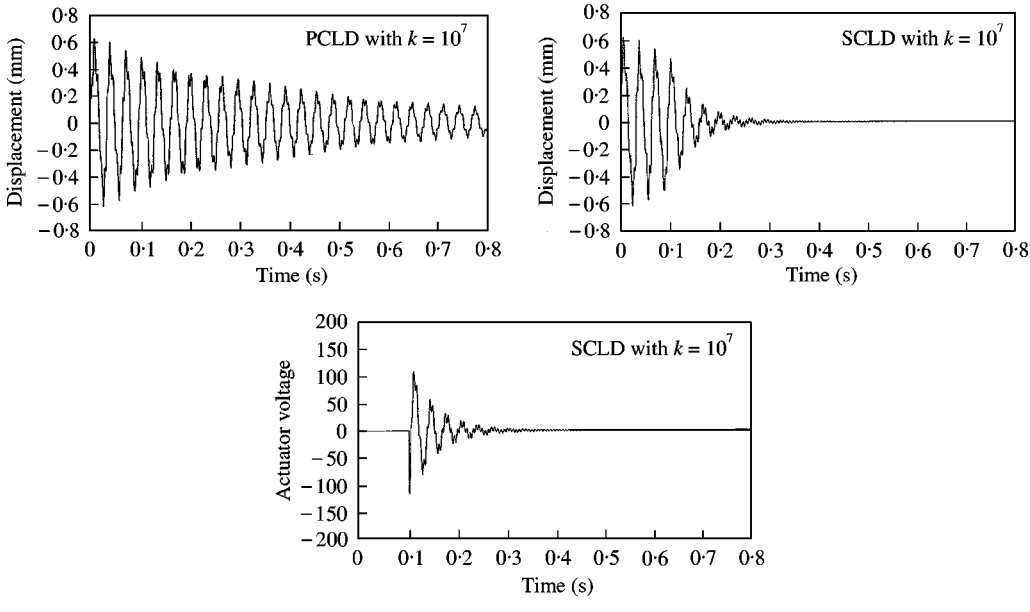

Figure 6. The frequency response of the beam with passive network (axis Y—absolute displacement, mm; axis X—frequency, Hz).

In order to study in detail the effect of the shear modulus (related to κ), the loss factor (related to α) and the thickness of the viscoelastic layer (t_s) on the vibration control performance, let us consider three aspects of the SCLD-treated systems, such as

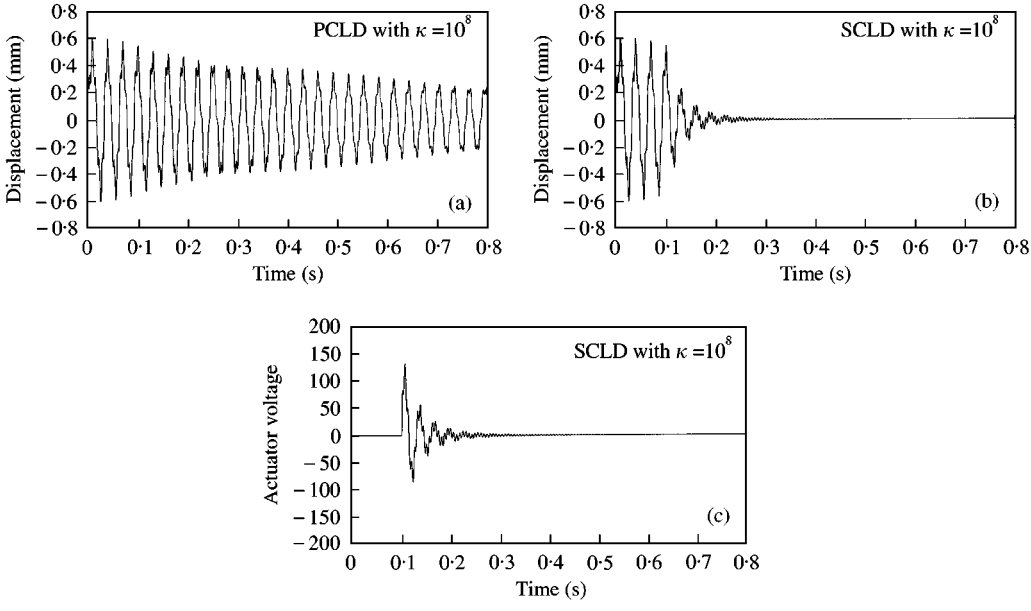

Figure 7. Tip displacement and actuator voltage of the beam with PCLD and SCLD (with $\kappa = 10^8$ N/m^2), when subjected to an impact load of 1·0 N at the tip.

passive damping ability, hybrid (combined) active–passive action ability and active action ability.

6.1. PERFORMANCE AND CONTROL EFFORT INDICES

To establish vibration control performance and control effort indices, the system is assumed to be subjected to a broadband extevrnal disturbance which is a white-noise process with zero mean.

$$E[u_d(t)] = 0, \qquad E[u_d(t)u_d^{\mathrm{T}}(\tau)] = U_d(t)\delta(t-\tau). \tag{60, 61}$$

The system response consists of a state vector with zero mean and a variance given by the solution $[P_l]$ of the Lyapunov equation

$$[A][P_l] + [P_l][A]^{\mathrm{T}} + \{\hat{B}\}\, U_d \{\hat{B}\}^{\mathrm{T}} = 0, \tag{62}$$

where

$$[P_l] = E[\{q(t)\}\ \{q(t)\}^{\mathrm{T}}]. \tag{63}$$

The output co-variance matrix can be written as

$$W = E[yy^{\mathrm{T}}] = E[[[C_o]\{q\}][[C_o]\{q\}]^{\mathrm{T}}] = E[[C_o]\{q\}\{q\}^{\mathrm{T}}[C_o]^{\mathrm{T}}]$$
$$= ([C_o]E[\{q\}\{q\}^{\mathrm{T}}][C_o]^{\mathrm{T}} = [C_o][P_l][C_o]^{\mathrm{T}}. \tag{64}$$

In this study, covariance response to white noise is observed. A random disturbance with intensity ($2{\cdot}5 \times 10^{-5}$ N^2/(rad/s)) is applied to the beam at the free end and the output $\{y\}$ is chosen to reflect the beam tip displacement.

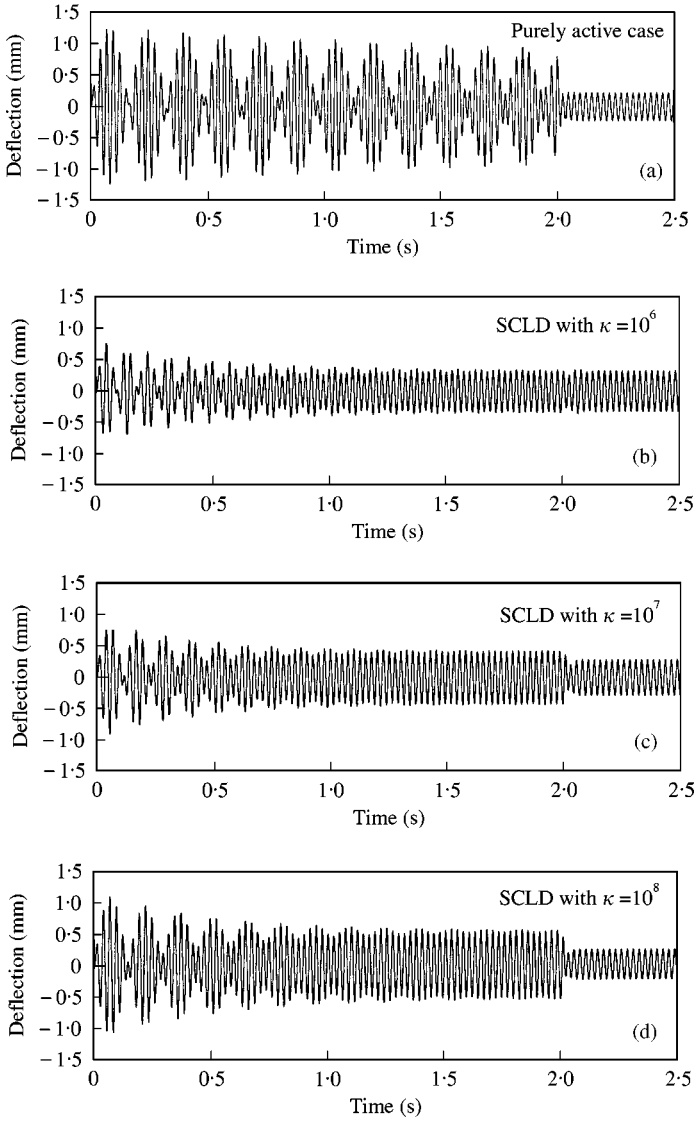

Figure 8. Tip displacement of the beam with purely active and SCLD (with $\kappa = 10^6$, 10^7 and 10^8 N/m^2), when subjected to a harmonic load of 0·1 sin (250t) N at the tip.

To obtain further insight, we define the standard deviations of the output vibration amplitude and the required voltage as σ_w and σ_v respectively. Here σ_w is an index representing the vibration suppression performance (the smaller σ_w, the better the performance) and σ_v is an index representing the required control effort.

6.2. PASSIVE DAMPING ABILITY

For a purely passive case ($V(t) = 0$), let $\sigma_w^{P_o}$ be the vibration suppression performance index for a case without viscoelastic damping (i.e., by removing GHM dissipation

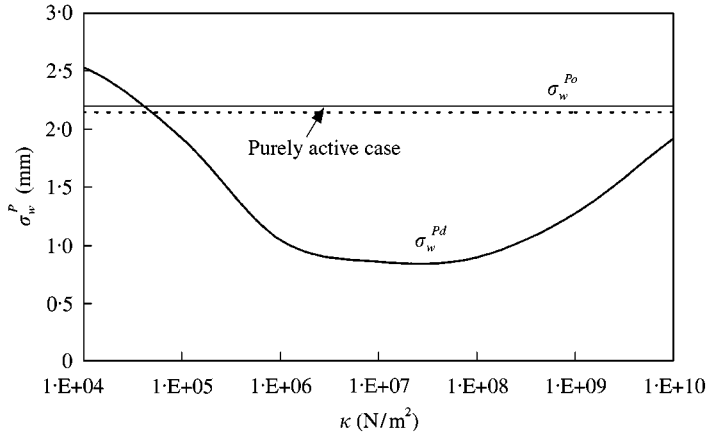

Figure 9. Standard deviation of tip displacement (σ_w^P) versus κ for PCLD case.

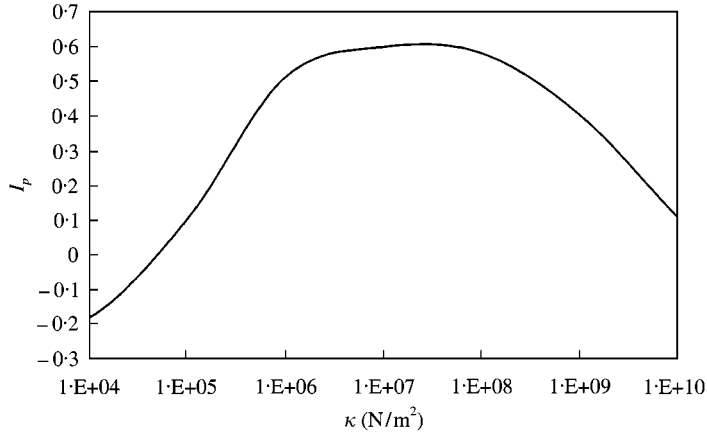

Figure 10. Passive damping ability (I_p) versus κ.

co-ordinates, retaining the viscoelastic stiffness contribution) and σ_w^{Pd} be the value with the viscoelastic damping. i.e., σ_w^{Po} and σ_w^{Pd} are obtained with the same system static stiffness for given κ. Figure 9 shows the variation of σ_w^P values with κ. It can be observed from the figure that, σ_w^{Po} remains constant and σ_w^{Pd} decreases with increase in κ. This indicates that the increase in the shear modulus increase the viscoelastic passive damping ability.

The passive damping ability of the viscoelastic material can be quantified with an index I_p defined as

$$I_p = \frac{\sigma_w^{Po} - \sigma_w^{Pd}}{\sigma_w^{Po}}. \tag{65}$$

Here $(\sigma_w^{Po} - \sigma_w^{Pd})$ can be considered as the vibration amplitude reduction due to viscoelastic damping. The variation of I_p with κ is illustrated in Figure 10. It can be noted that viscoelastic passive damping ability on the SCLD system increases with κ upto certain level and afterwards decreases with further increase in κ.

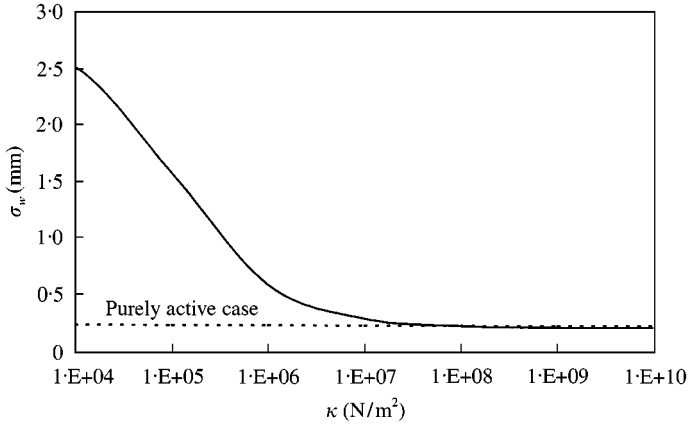

Figure 11. Standard deviation of tip displacement (σ_w) versus κ for a hybrid case with both active and passive actions.

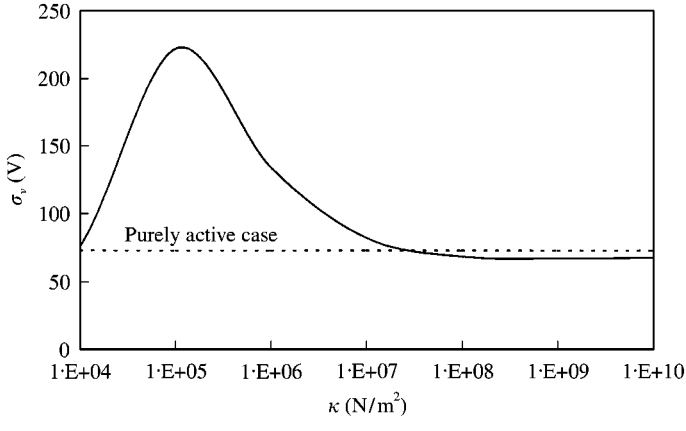

Figure 12. Standard deviation of tip actuator voltage (σ_v) versus κ for a hybrid case with both active and passive actions.

6.3. HYBRID ACTIVE–PASSIVE ACTIONS

The foregoing discussion revealed the capability of the SCLD-treated system in providing a significant level of passive damping ability. Now let us consider the overall closed-loop system performance combining the active and passive actions. For this study, a while-noise disturbance with zero mean and with variance 2.5×10^{-5} N^2/(rad/s) is applied at the tip (free end) of the beam and the output is chosen to be the transverse displacement of the beam at the tip. This results in the corresponding state-space equations to be single-input–single-output system (SISO) with the weighting matrices Q and R as scalars.

The structure response index σ_w and corresponding control effort index σ_v are shown in Figures 11 and 12. It can be noted that, in this example, the SCLD configuration with lower value of κ needs more control voltage while achieving less vibration reduction when compared to a purely active system. With increase in the κ the vibration amplitude and the required control effort decreases. Moreover, with sufficiently large κ, SCLD marginally

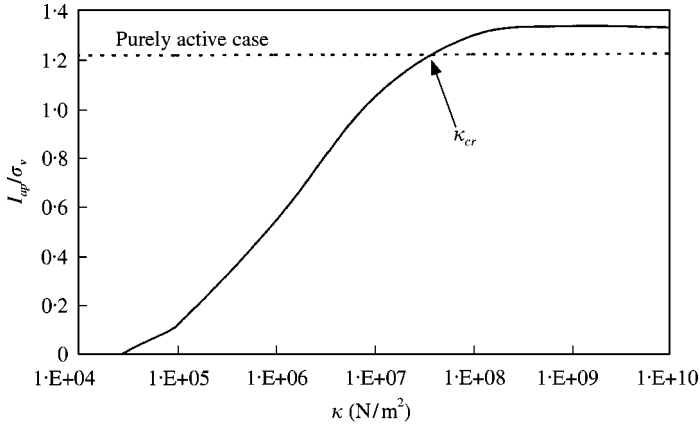

Figure 13. Vibration suppression ability per control effort (I_{ap}/σ_v) versus κ for a hybrid case with both active and passive actions.

outperforms the purely active system. Another index which represents the active–passive hybrid action quantitatively, I_{ap}, could be defined as

$$I_{ap} = \frac{\sigma_w^{P_o} - \sigma_w}{\sigma_w^{P_o}} \times 100. \tag{66}$$

Here, $(\sigma_w^{Po} - \sigma_w)$ can be considered as the vibration amplitude reduction due to contributions from the active–passive hybrid actions. (I_{ap}/σ_v) represents the vibration suppression ability per control effort, which represents the effectiveness of the active–possible hybrid actions. The (I_{ap}/σ_v) are plotted for various values of κ in Figure 13. The κ value at which (I_{ap}/σ_v) value of SCLD is larger than that of a purely active case will yield a design that outperforms both purely active and passive designs. The κ value at which (I_{ap}/σ_v) value is crossing the dashed line could be defined as κ_{cr}. If the viscoelastic shear layer with κ more than κ_{cr} is provided in SCLD design, it will outperform the purely active and passive designs. However, in general, large values of κ are difficult to achieve and maintain in most viscoelastic materials.

It can be noted that the shape of these curves depends on the control parameters Q and R chosen. For instance, as the value of Q increases values of κ_{cr} (the value of κ related to shear modulus) required for the SCLD design to outperform purely active case, will obviously increase, because we demand more vibration suppression which demands more active action. This is clearly indicated in Figures 14–16. But qualitatively the dependence of κ and α on the control performance is similar for various values of Q and R.

The vibration response index σ_w for various values of α (related to loss factor) for PCLD and SCLD cases are indicated in Figure 17. It can be seen that it is desirable to let the value of α as large as possible to achieve better vibration control. Vibration suppression ability per control effort (I_{ap}/σ_v) versus κ and α is plotted in Figure 18. The parametric region in which the I_{ap}/σ_v value of SCLD design is larger than that of purely active design gives a design that outperforms the purely active and passive designs. Figure 19 shows the variation of σ_w with respect to the viscoelastic layer thickness (t_s). It can be noted that the larger the thickness of the viscoelastic layer the lesser will be the vibration control performance. This is due to the reduction in the transmissibility of the active action from the smart layer to the host structure by the viscoelastic layer. This can be clearly brought out by defining another parameter called the active action authority (I_a).

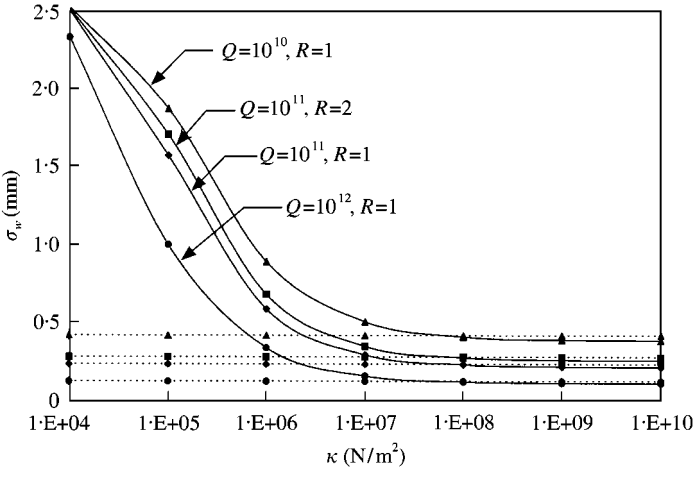

Figure 14. Standard deviation of tip displacement (σ_w) versus κ for a hybrid case with both active and passive actions for different values of control parameters Q and R. *Note*: The dotted lines indicate the corresponding purely active cases.

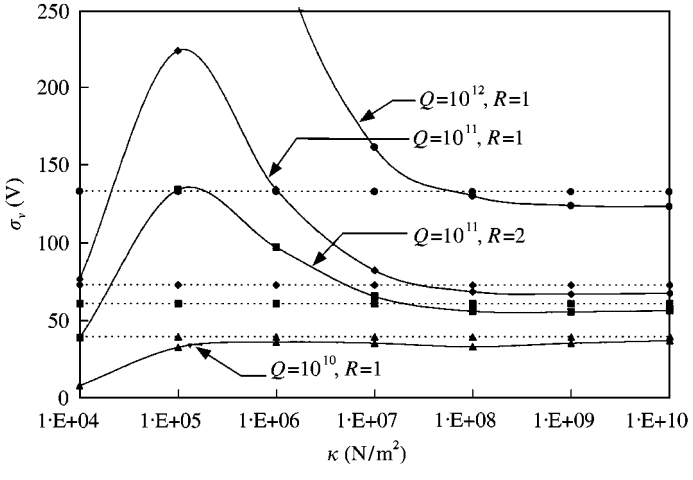

Figure 15. Standard deviation of the actuator voltage (σ_v) versus κ for a hybrid case with both active and passive actions for different values of control parameters Q and R. *Note*: The dotted lines indicate the corresponding purely active cases.

6.4. ACTIVE ACTION AUTHORITY

To study the active action authority without damping effect, the structure is statically deformed by a DC voltage input to the actuator. The beam deflection at the tip is further transformed to an equivalent point load by multiplying it by the equivalent beam stiffness at the tip. The transmitted force per unit input voltage is then normalized with respect to that of the purely active system, which is defined as

$$I_a = \left(\frac{w_v}{w_F}\right) \Big/ \left(\frac{w_v}{w_F}\right)_{PA}, \tag{67}$$

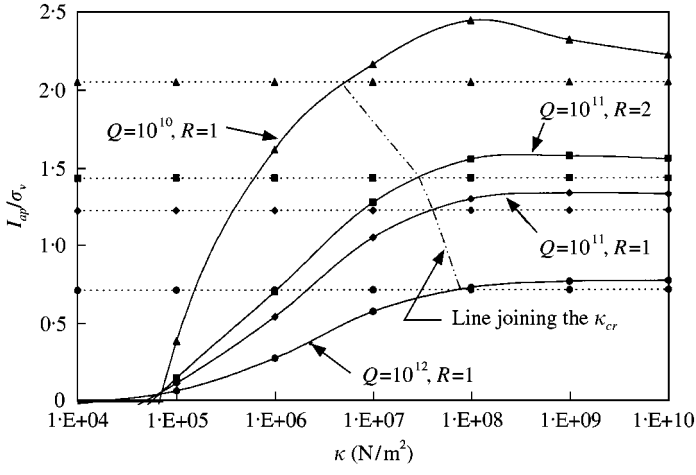

Figure 16. Vibration suppression ability per control effort (I_{ap}/σ_v) versus κ for a hybrid case with both active and passive actions for different values of control parameters Q and R. *Note*: The dotted lines indicate the corresponding purely active cases.

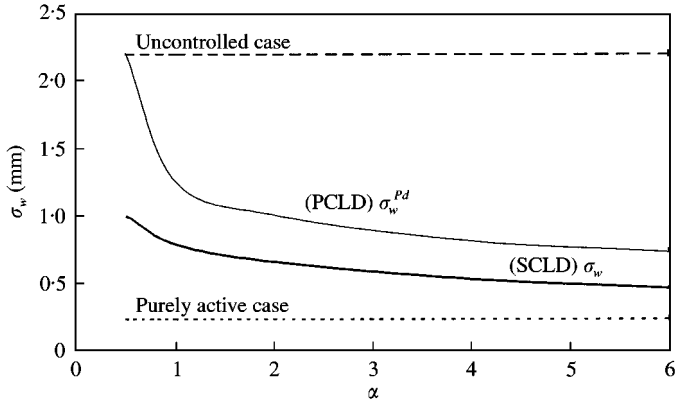

Figure 17. Standard deviation of tip displacement (σ_w) versus α for a hybrid case with both active and passive actions (for $\kappa = 5{\cdot}0 \times 10^5$ N/m^2).

where w_v is the static deflection at the free end when unit DC input voltage is applied to the actuator, and w_F is the beam tip deflection when unit force in transverse direction is applied to the beam at the free end. The subscript PA refers to the purely active system. Higher I_a indicates higher authority of the active action.

The difference in I_a can be due to two factors, namely the *transmission path* (the path along which the active action is transmitted to the host structure) and the *offset* (the distance between the neutral axis of the beam and that of the piezoelectric cover sheet).

The I_a values for different κ are plotted against t_s in Figure 20. It may be noted that purely active system is the case with $t_s = 0$. From the figure, we see that I_a increases with increasing κ for the same t_s (same offset). This shows that the shear modulus (proportional to κ) of the viscoelastic material is a key factor in the active action authority of the SCLD configuration. It is also illustrated that the I_a value for typical $\kappa's (\kappa < 10^8$ Pa) reduces significantly as t_s increases from 0. This phenomenon indicates that the active action is degraded by the viscoelastic layer. The reason for this is that the soft viscoelastic layer

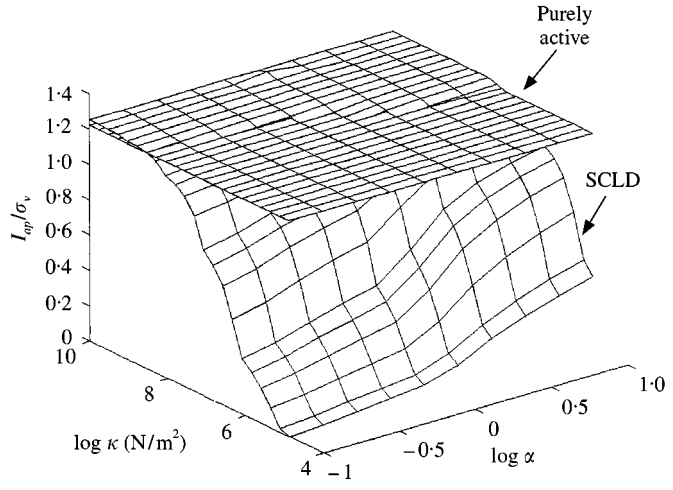

Figure 18. Vibration suppression ability per control effort (I_{ap}/σ_v) versus κ and α.

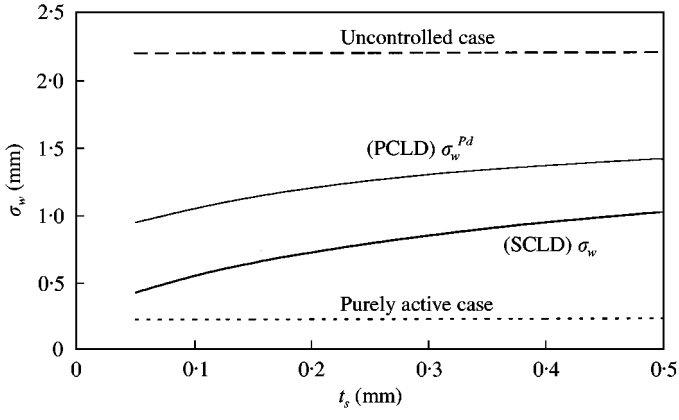

Figure 19. Standard deviation of tip displacement (σ_w) versus t_s for a hybrid case with both active and passive actions (for $\kappa = 5{\cdot}0 \times 10^5$ N/m^2).

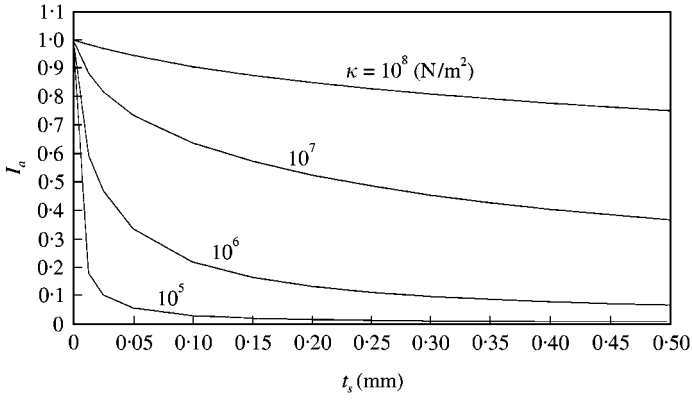

Figure 20. Active action authority (I_a) versus thickness of the viscoelastic shear layer (t_s) for different values κ.

TABLE 2

Comparison of the beam responses and control effort requirements for a broadband excitation

Standard deviation of	Beam response σ_w (mm)	Control voltage σ_v (V)
PCLD ($\kappa = 10^6$ N/m^2)	1·050000	—
SCLD ($\kappa = 10^6$ N/m^2)	0·586009	134·29471
PCLD ($\kappa = 10^7$ N/m^2)	0·862403	—
SCLD ($\kappa = 10^7$ N/m^2)	0·289847	82·53952
PCLD ($\kappa = 10^8$ N/m^2)	0·899485	—
SCLD ($\kappa = 10^8$ N/m^2)	0·227955	68·85565
Purely active	0·230805	73·21550

reduces the control authority being transmitted (transmissibility between the voltage input to the actuator and the force/moment applied on the structure) from the piezoelectric actuator to the host structure. For such cases, the active action authority decreases with increasing viscoelastic material thickness even though the offset distance is increased.

6.5. RESPONSE TO BROADBAND EXCITATION

To indicate the importance of the SCLD design over the PCLD and purely active designs, the standard deviation of the beam response and the required control voltage under broadband disturbance are shown in Table 2. It can be noted that there is improved performance (i.e., more vibration reduction) in the case of the SCLD design when compared to the PCLD design. With the SCLD design having viscoelastic layer of sufficient shear modulus (related to κ), more vibration reduction can be obtained with less control effort than the purely active design. However, large κ values ($\kappa > 10^8$) are in general too high to achieve and maintain in most viscoelastic materials.

7. CONCLUSIONS

A finite element model has been developed for the beam-like structure with partially covered, smart constrained layer damping (SCLD) treatment. The mechanics of the viscoelastic material layer is modelled using GHM approach, which is a time domain formulation. LQR optimal control has been applied to study the vibration control performance. It is observed that the SCLD with sufficiently large shear modulus (related to κ) could outperform both PCLD and purely active configurations. We could also estimate the required critical κ necessary for the SCLD systems. However, as large values of κ are difficult to achieve and maintain in most viscoelastic materials, a compromise has to be made in the choice of suitable κ keeping in mind that SCLD designs are more reliable, robust and fail-safe when compared to purely active designs. It is possible to work out the parametric design space (as in Figure 18) for the SCLD with optimal performance needs.

REFERENCES

1. S. S. RAO and M. SUNAR 1994 *Applied Mechanics Review* **47**, 113–123. Piezoelectricity and its use in disturbance sensing and control of flexible structures: a survey.

2. C. Q. CHEN and Y. P. SHEN 1997 *Smart Material and Structures* **6**, 403–409. Optimal control of active structures with piezoelectric modal sensors and actuators.
3. K. Y. LAM and T. Y. NG 1999 *Smart Materials and Structures* **8**, 223–227. Active control of composite plates with integrated piezoelectric sensors and actuators under various dynamic loading conditions.
4. I.Y. SHEN 1994 *American Society of Mechanical Engineers Journal of Vibration and Acoustics* **116**, 341–349. Hybrid damping through intelligent constrained layer treatments.
5. I. Y. SHEN 1996 *American Society of Mechanical Engineers Journal of Vibration and Acoustics* **118**, 70–77. Stability and controllability of Euler–Bernoulli beams with intelligent constrained layer treatments.
6. A. BAZ and J. RO 1994 *Sound and Vibration Magazine* **28**, 18–21. The concept and performance of active constrained layer damping treatments.
7. A. BAZ and J. RO 1995 *American Society of Mechanical Engineers Special* 50*th Anniversary Design Issue* **117**, 135–144. Optimum design and control of active constrained layer damping.
8. J. A. RONGONG, J. R. WRITE, R. J. WYNNE and G. R. TOMLINSON 1997 *American Society of Mechanical Engineers Journal of Vibration and Acoustics* **119**, 120–130. Modelling of a hybrid constrained layer/piezoceramic approach to active damping.
9. J. M. YELLIN and I. Y. SHEN 1996 *Smart Materials and Structures* **5**, 628–637. A self-sensing active constrained layer damping treatment for a Euler–Bernoulli beam.
10. W. H. LIAO and K. W. WANG 1997 *American Society of Mechanical Engineers Journal of Vibration and Acoustics* **119**, 563–572. On the active–passive hybrid control actions of structures with active constrained layer treatments.
11. *IEEE Standard on Piezoelectricity* 1987 ANSI-IEEE Std 176–1987.
12. R. M. CHRISTENSEN 1982 *Theory of Viscoelasticity*: *An Introduction*. New York: Academic Press; second edition.
13. D. F. GOLLA and P. C. HUGHES 1985 *American Society of Mechanical Engineers Journal of Applied Mechanics* **52**, 897–906. Dynamics of viscoelastic structures—a time domain finite element formulation.
14. D. J. MCTAVISH and P. C. HUGHES 1993 *American Society of Mechanical Engineers Journal of Vibration and Acoustics* **115**, 103–110. Modelling of linear viscoelastic space structures.
15. K. J. BATHE 1996 *Finite Element Procedures in Engineering Analysis*. Englewood Cliffs, NJ: Prentice-Hall.
16. H. KWAKERNAAK and R. SIVAN 1972 *Linear Optimal Control Systems*. New York: John Wiley and Sons, Inc.
17. K. OGATA 1994 *Designing Linear Control Systems with Matlab*. Englewood Cliffs, NJ: Prentice-Hall.
18. W. T. THOMSON 1988 *Theory of Vibration with Application*. Englewood Cliffs, NJ: Prentice-Hall; third edition.

APPENDIX A: NOMENCLATURE

$[A]$	open-loop system matrix
$[A_{cl}]$	closed-loop system matrix
A_b, A_c, A_s	cross-sectional are a of beam, piezoelectric layer and viscoelastic material respectively
$[B]$	control matrix
$[\hat{B}]$	disturbance matrix
b	width of the beam
$[C]$	global damping matrix
$[C_z]$	damping matrix corresponding the z dissipation co-ordinate of viscoelastic material
$[\bar{C}]$	global damping matrix in modal co-ordinates
$[C_b]$	Rayleigh damping matrix
$[C_o]$	output matrix
D	electrical displacement
d_{31}	piezoelectric constant
E	electric field
E_b, E_c	Young's modulus of beam material and piezoelectric material respectively

$\{P_c\}$	control force vector
$\{\bar{P}_c\}$	control force vector in modal co-ordinates
$\{f_d\}$	disturbance force vector
$\{\bar{f}_d\}$	disturbance force vector in modal co-ordinates
G	relaxation function of viscoelastic material
G_b, G_c	shear modulus of the beam material and piezoelectric material respectively
I_b, I_c, I_s	moment of inertia of beam, piezoelectric constraining layer and viscoelastic shear layer respectively
$[K]$	global stiffness matrix
$[K_z]$	stiffness matrix corresponding the z dissipation co-ordinate of viscoelastic material
$[K_{qz}]$	stiffness matrix coupling z dissipation co-ordinate of viscoelastic material and displacement co-ordinates of the beam
$[\bar{K}]$	global stiffness matrix in modal co-ordinates
k_{eq}	equivalent stiffness of edge element
L	beam length
L_e	element length
$[M]$	global mass matrix
$[M_z]$	mass matrix corresponding the z dissipation co-ordinate of viscoelastic material
$[\bar{M}]$	global mass matrix in modal co-ordinates
$\{q\}$	global displacement vector
S_{11}^E	elastic compliance constant of piezoelectric materials
t	time
t_b, t_c, t_s	thickness of beam, piezoelectric constraining layer and viscoelastic shear layer respectively
$\{u\}$	control input vector
$\{u_d\}$	disturbance input vector
u_b, u_c, u_s	axial displacement of beam, piezoelectric layer and viscoelastic layer respectively
V	applied actuator voltage
w	beam transverse displacement
$[N_w],[N_\theta],[N_u],[N_\gamma]$	shape function matrices for transverse displacement, rotation, axial displacement of the beam and rotation of the viscoelastic layer
x	position co-ordinate along beam and element length
$[N_z]$	shape function matrix for dissipation co-ordinate
x_1	left end of SCLD
x_2	right end of SCLD
$\{y\}$	output vector
z	dissipation co-ordinate
α	weighting on GHM dissipation co-ordinate (related to loss factor)
γ	shear strain of viscoelastic material
E	mechanical strain of viscoelastic material
ε_{33}^T	dielectric constant of piezoelectric material
κ	final value of $G(t)$ (related to shear modulus)
ζ	damping factor in GHM dissipation co-ordinate
ρ_b, ρ_c, ρ_s	mass density of beam material, piezoelectric material and viscoelastic material respectively
τ	mechanical shear stress
θ	rotation of the beam
ψ	rotation of the viscoelastic layer
$\hat{\omega}$	natural frequency of GHM dissipation co-ordinate
$\hat{\phi}$	truncated modal matrix
η	modal co-ordinates
k_α	shear correction factor (= 5/6)
$[K_c]$	gain matrix
$\{\xi\}$	state vector
I_a	active action authority index
I_p	passive damping ability index
I_{ap}	active–passive damping ability index
σ_w	standard deviation of the transverse displacement
σ_w^P	standard deviation of the transverse displacement for a passive case
σ_v	standard deviation of the control effort